Electronic Supplementary Material (ESI) for Journal of Materials Chemistry A.

Supporting Information

Proton-Mediated Energy Storage in Intermediate-Temperature Solid-Oxide Metal-Air Battery

*Nansheng Xu, Cuijuan Zhang and Kevin Huang**

Department of Mechanical Engineering, University of South Carolina,

Columbia, SC 29208 United State

*E-mail: HUANG46@cec.sc.edu

Experimental Section

Materials preparation: The functional energy storage medium (ESM) materials for this study contain two phases, Fe and a Fe-supporting oxide (SO) phase, which varies from ZrO_2, $BaZr_{0.8}Y_{0.2}O_{2.9}$ (BZY20) and $BaCe_{0.7}Zr_{0.1}Y_{0.1}Yb_{0.1}O_{3-\delta}$ (BCZYYb). The SO phase was prepared by a citric acid-nitrate method with $ZrO(NO_3)_2 \cdot xH_2O$ (99%, Sigma-Aldrich), $Ba(NO_3)_2$ (99.0%, Alfa Aesar), $Y(NO_3)_3 \cdot 6H_2O$ (99.9%, Alfa Aesar), $Ce(NO_3)_3 \cdot 6H_2O$ (99.5%, Alfa Aesar) and $Yb(NO_3)_3 \cdot 5H_2O$ (99.9%, Sigma-Aldrich) as metal precursors. Briefly, ZrO_2 was synthesized by dissolving 0.05 mol of $ZrO(NO_3)_2 \cdot xH_2O$ into an acid solution containing nitric acid (70%, Sigma-Aldrich) and water in a volume ratio of 1:9. Then citric acid (99.5%, Sigma-Aldrich) was added with molar ratio to metal ions of 2:1. After stirring for several hours, pH of the solution was adjusted to ~ 6 by adding ammonia (28-30%, BDH), followed by heating on a hot plate until auto-ignition. The as-prepared powders were then well grounded and heat-treated at 1200 ^oC in air for 5 h. The BZY20 and BCZYYb powders were prepared by the similar method.

The active metal Fe was first introduced into the SO phase (ZrO_2 or BZY20 or BCZYYb) in the form of Fe_2O_3 by a simple incipient wetness impregnation of $Fe(NO_3)_3 \cdot 9H_2O$ as the precursor[1]. The weight ratio between the SO and Fe_2O_3 was set to be 5:5. Briefly, a 0.5 g fine, SO powders were weighted, followed by adding 2.53 g $Fe(NO_3)_3 \cdot 9H_2O$ with DI water as solvent. After intimate grinding and drying, the SO powders were coated with a thin layer of $Fe(NO_3)_3$. Then the powders were heat-treated at 600 ^oC in air for 2h to obtain Fe_2O_3-coated SO (ZrO_2 or BZY20 or BCZYYb) powders.

Fabrication of anode-supported SOFC: The anode supported solid oxide fuel cells use $(ZrO_2)_{0.89}(Sc_2O_3)_{0.1}(CeO_2)_{0.01}$ (10Sc1CeSZ), Ni-10Sc1CeSZ, $LaSrMnO_3$/ $(Bi_{0.75}Y_{0.25})_{0.93}Ce_{0.07}O_{1.5}$ (LSM-BYC7) as electrolyte, anode, and cathode, respectively. Firstly, the anode supported half cells were prepared by co-pressing and co-sintering method, while, the LSM-BYC7 cathode material of RSOFC and was prepared by a citric acid-nitrate method, which can be found in details in our previous work[1, 2]. Briefly, NiO (J.T. Baker) and 10Sc1CeSZ (Daiichi Kigenso Kagaku Co. Ltd., Japan) with weight ratio of 70:30 were ball-milled for 12 h in ethanol medium. The obtain slurry was dried at 80 ^oC oven and then well ground with 2 wt.% carbon lampblack (Fisher Chemical) as pore former and 2 wt.% polyvinyl butyral (PVB, Butvar® B-98, Sigma) as binder. Then, the obtained powders were pressured into pellets of 1 inch in diameter. Then the 10Sc1CeSZ powder was distributed uniformly onto the surface of the anode pellet, followed by co-pressing with the anode substrate to form bi-layers. The pellets were then co-sintered at 1300 ^oC for 5 h. The LSM-BYC7 cathode ink, with a weight ratio of LSM:BYC7:V-006A (Heraeus, USA) = 40:60:100, was screen-printed onto the surface of electrolyte and baked at 800 oC for 2 h to form the single cell. The effective area of electrode is 1.267 cm^2. Silver mesh and paste were used as current collector. The detail information about the cathode material preparation and fuel cell fabrication can be found in our previous work [1, 2].

Battery construction and test: 0.157 g of Fe_2O_3 coated SO powders were loaded into anode chamber. Single RSOFC was placed on the top of the chamber, followed by sealing with glass (Schott, GM31107). The performance of battery was examined on a multichannel Solartron electrochemical station (1260 frequency response analyzer + 1287 potentiostat). The battery was first heated in air from room temperature to 650 ^oC to melt the sealing

glass. The temperature was then decreased to 550 ^{o}C in a rate of 2 ^{o}C/min and a flow of H_2/3%H_2O (50 SCCM) were introduced to the chamber to reduce the NiO to Ni in the anode and Fe_2O_3 to Fe in the ESM material. Once the reduction was complete, both the fuel gas outlet and inlet were closed in sequence and the open circuit voltage was monitored until it reached equilibrium, around the theoretical potential of 1.067 V for the Fe-Fe_3O_4 redox couple at 550 ^{o}C. Now the battery was ready for discharge/charge cycle.

Temperature programmed reduction (TPR) characterization: The reduction activity of Fe_2O_3-SO materials was examined by TPR using a Micromeritics Autochem II 2920 chemisorption analyzer. Approximately 45 mg of powders was loaded into the sample tube and pre-treated at 300 ^{o}C for 1 h in He at a flow rate of 50 sccm to remove the adsorbed moisture. The samples were cooled down to room temperature and then heated from room temperature to 900 ^{o}C at a ramping rate range of 2.5-15 ^{o}C min^{-1} and then held at 900 ^{o}C for 1 h in 5%H_2/N_2 at a flow rate of 50 sccm. The consumed hydrogen was analyzed by a thermal conductivity detector (TCD). For comparison, TPR of pure BCZYYb was also carried out. However, the TPR profiles of BCZYYb represent the lattice oxygen release to form the oxygen vacancies process, as described by [3]

$$O_O^{\times} + 2Ce_{Ce}^{\times} \rightarrow V_O^{\bullet\bullet} + 2Ce_{Ce}^{'} + \frac{1}{2}O_2\,(g) \qquad \text{(S1)}$$

Other characterization: The morphology of SO and Fe_2O_3-coated SO samples before test was characterized by field-emission scanning electron microscopy (FESEM, Zeiss Ultra plus). The phases in the SO, Fe_2O_3-coated SO and post-reduced Fe_2O_3-coated-SO were examined by X-ray diffraction (XRD) using a MiniFlexTM II bench-top XRD system diffractometer (Rigaku Corporation, Japan).

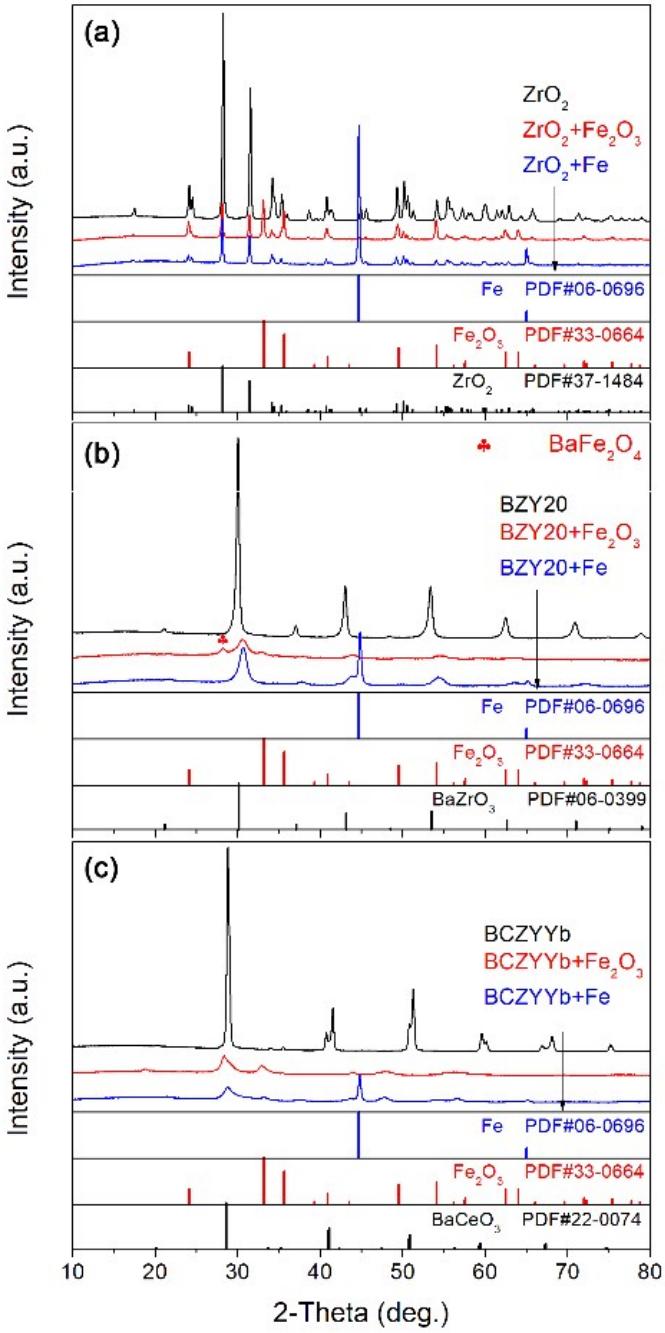

Figure S1. XRD patterns of as-prepared SO, Fe_2O_3-coated SO and post-reduced Fe_2O_3-coated-SO (a) ZrO_2; (b) BZY20; (c) BCZYYb

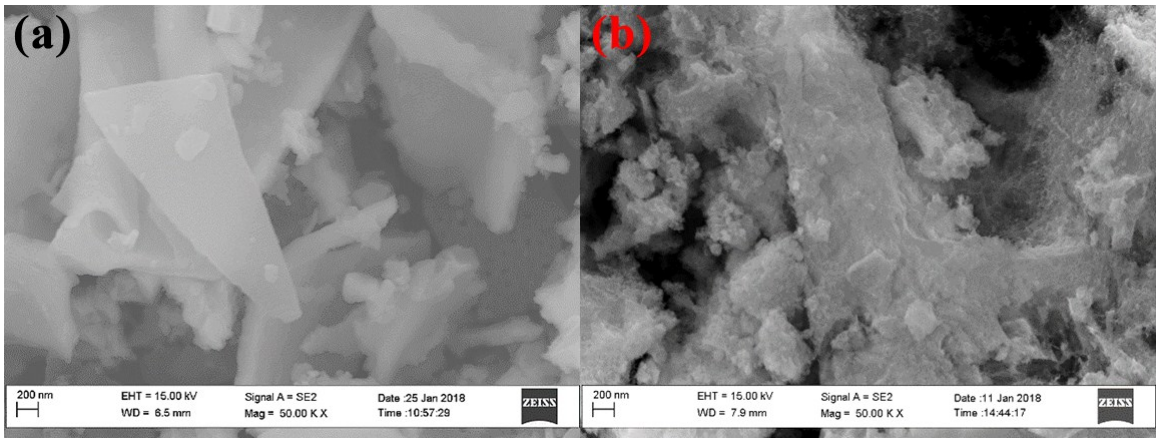

Figure S2. Morphologies of (a) SO and (b) Fe_2O_3-coated SO.

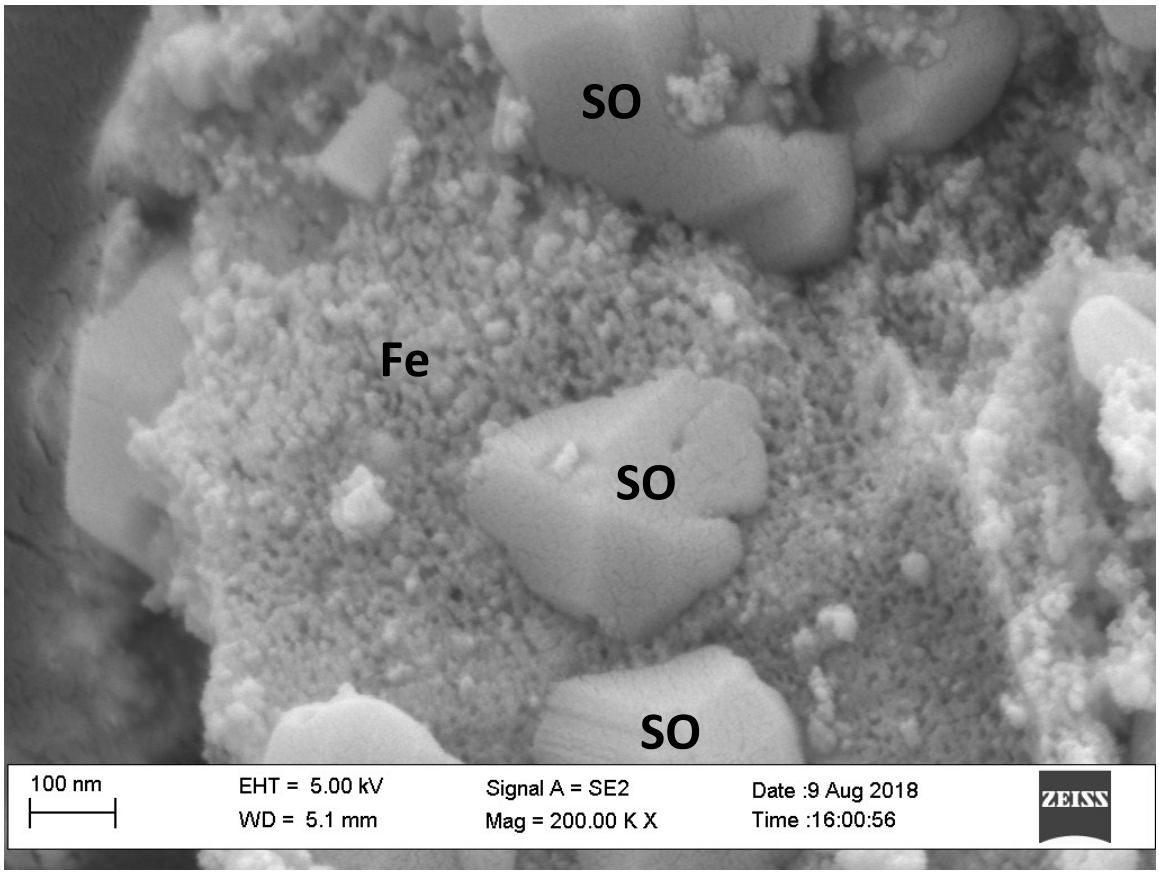

Figure S3. Morphologies of post-reduced Fe_2O_3-coated SO.

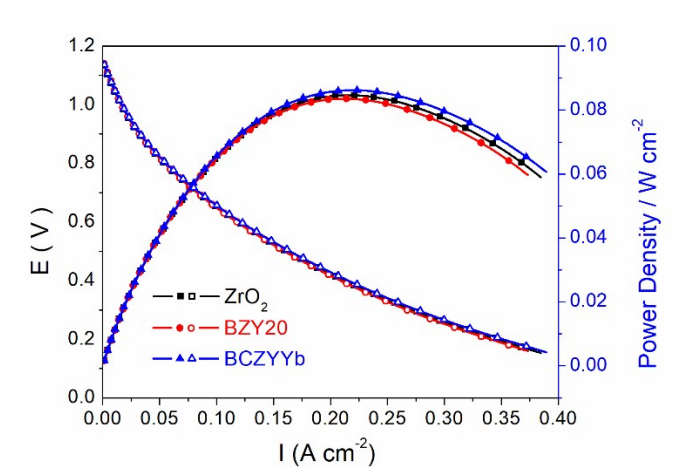

Figure S4. Cell performances of each cell.

The almost identical V-I curves for batteries with difference ESM suggest that the performance differences shown in Fig. 1-3 are solely related to the ESM.

The kinetic of the reduction process of Fe_2O_3 to Fe can be investigated by TPR method[4]. With varying the ramping rate, the peak temperature on the TPR profile would be different. The peak temperature T_{max}, active energy E of the reduction process and ramping rate φ follows the relationship as described by

$$\ln\left(\frac{\varphi}{T_{max}^{2}}\right) = -\frac{E}{RT_{max}} - \ln\left(\frac{E}{AR}\right) + C \qquad \text{(S2)}$$

where A is the pre-exponential term; R is the universal gas constant. By plotting $\ln\left(\frac{\varphi}{T_{max}^{2}}\right)$ against $\frac{1}{T_{max}}$ yields a straight-line, from whose slope the activation energy E of the reduction process can be obtained. The detailed derivation of eq (S2) can be found in reference [4].

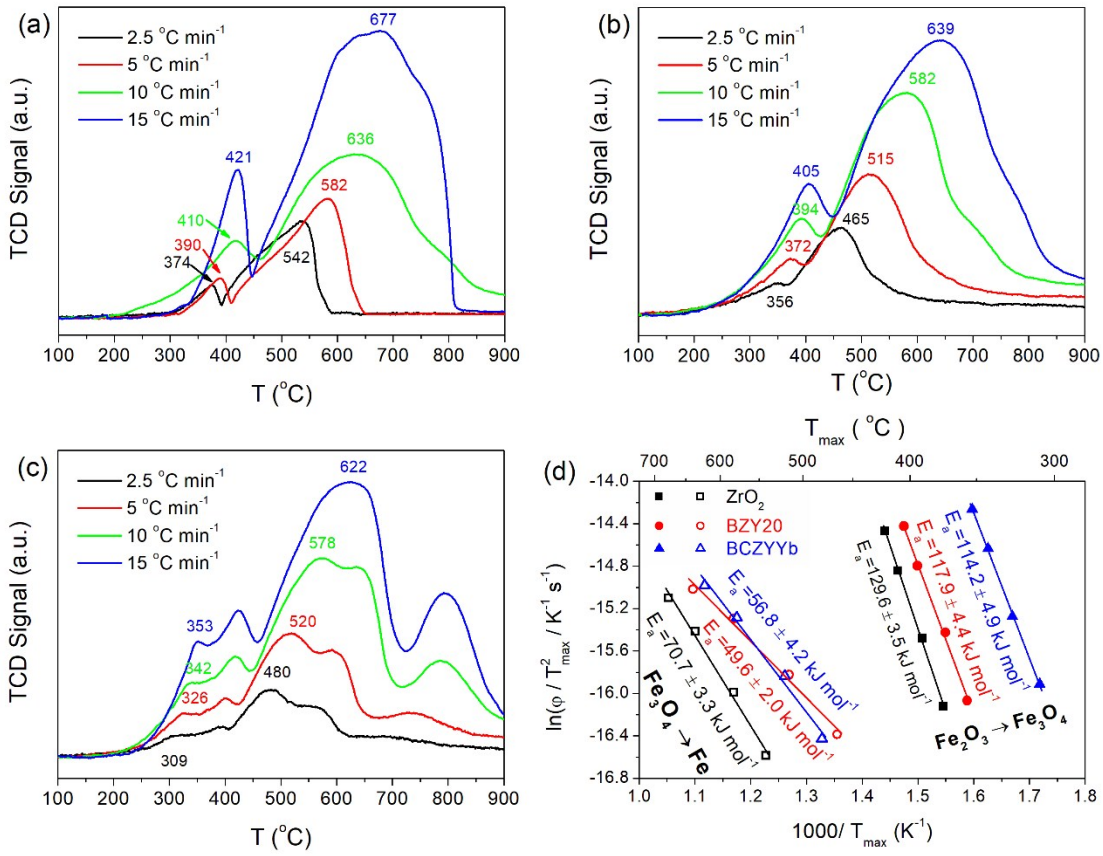

Figure S5. TPR profiles under different ramping rates for (a)Fe_2O_3/ZrO_2; (b)Fe_2O_3/BZY20; (c)Fe_2O_3/BCZYYb; (d) Temperature-programmed Arrhenius plots.

As shown in Fig S5, the reduction of Fe_2O_3 to Fe contains two steps. The first step is related to the reduction from Fe_2O_3 to Fe_3O_4, corresponding to the low-temperature peak in Fig S5. The high-temperature peak is associated with the second step of the reduction, from Fe_3O_4 to Fe.

From the slopes shown in Fig S5d, the active energies of these two reduction steps of each ESM were calculated and listed. The activation energies for the first-step reduction are 129.6, 117.9 and 114.2 kJ mol^{-1} for Fe_2O_3/ZrO_2, Fe_2O_3/BZY20 and Fe_2O_3/BCZYYb, respectively, while they are 70.7, 49.6 and 56.8 kJ mol^{-1} for the second-step reduction for Fe_2O_3/ZrO_2, Fe_2O_3/BZY20 and Fe_2O_3/BCZYYb, respectively. Clearly, the use of proton-containing ceramics as the SO media can decrease the active energy of each reduction step, thus improve the kinetic rate of the reduction process.

References:

1. C. Zhang and K. Huang, *ACS Energy Letters*, 2016, **1**, 1206-1211.
2. C. Zhang and K. Huang, *Journal of Power Sources*, 2017, **342**, 419-426.
3. S. Ricote, A. Manerbino, N. P. Sullivan and W. G. Coors, *Journal of Materials Science*, 2014, **49**, 4332-4340.
4. H.-Y. Lin, Y.-W. Chen and C. Li, *Thermochimica Acta*, 2003, **400**, 61-67.